



# Soft Matter

## **Roughness Tolerant Pressure Sensitive Adhesives made of Sticky Crumpled Sheets**

Journal:	<i>Soft Matter</i>
Manuscript ID	SM-ART-06-2022-000858.R2
Article Type:	Paper
Date Submitted by the Author:	29-Sep-2022
Complete List of Authors:	Elder, Theresa; North Dakota State University, Materials and Nanotechnology Croll, Andrew; North Dakota State University, Physics

SCHOLARONE™  
Manuscripts

Cite this: DOI: 00.0000/xxxxxxxxxx

# Roughness Tolerant Pressure Sensitive Adhesives made of Sticky Crumpled Sheets<sup>†</sup>

Theresa Elder,<sup>a</sup> and Andrew B. Croll<sup>\*a,b</sup>

Received Date

Accepted Date

DOI: 00.0000/xxxxxxxxxx

If an adhesive is meant to be temporary, roughness often poses a challenge for design. An adhesive could be made soft so that it can deform and increase surface contact but a softer material will in general hold a smaller load. Bioinspired adhesives, made with numerous microscale posts, show promise as roughness tolerant adhesives but are complicated to fabricate. In this work, we show how thin polymer sheets, when crumpled into a roughly spherical shape, form a very simple and roughness tolerant adhesive system. We use micro and macro-scale experiments to measure adhesion forces between various substrates and crumpled polydimethylsiloxane sheets. We find the force-displacement curves resemble probe-tack experiments of traditional pressure sensitive adhesives and that moderate tensile forces are required to initiate interfacial failure. Notably, we see that sticky crumples often perform better on long wavelength roughness than they do on smooth substrates. In order to improve the peak pull-off forces, we create a sticky crumple from a thin sheet of a glassy polymer, polycarbonate, coated with an adhesive layer. This elasto-plastic sticky crumple achieves high pull-off forces even on the rough surface of a landscaping brick.

## 1 Introduction

Depending on their makeup and intended uses, adhesives can be organized into one of several categories and will respond to substrate roughness in a variety of ways. For example, a structural adhesive is an adhesive that is typically used to join two load-bearing pieces of a structure together.<sup>1,2</sup> Structural adhesives typically benefit if a substrate is roughened prior to application because they are often designed to wet and flow around roughness and then cure to a solid state.<sup>3</sup> This kind of bonding maintains the high loads required by structural applications because both contact area and bond rigidity are maximized.

On the other hand, some applications like attaching a poster to a wall, require non-permanent bonding. In this case, a pressure sensitive adhesive (PSA) might be used. PSAs are often viscoelastic materials, and so can flow around some small scale roughness with an applied pressure.<sup>4</sup> They dissipate energy during pull-off, and typically reach much lower peak loads before failure because of their low stiffness.<sup>5</sup> One could say that a PSA is defined as a high-loss, viscoelastic, low peak force adhesive. Larger scale roughness (Fig. 1) is usually a problem for a PSA because they are not intended to flow on large scales upon application (typically a residue after removal is considered undesirable). The result is a vastly decreased amount of contact and a much weaker adhesion

overall for PSAs on rough substrates.<sup>6</sup>

Interestingly, many naturally occurring organisms have adhesive systems which can achieve both high peak forces and are still easily removable, even on rough substrates.<sup>7-14</sup> In many cases, specialized stiff, hierarchical structures have evolved to facilitate the adhesion. Because the structures are slender, they are easily bent around substrate roughness but maintain stiffness along their length. Different levels of the hierarchy deform to accommodate different scales of roughness. To remove the adhesion, the organism simply peels the adhesive structures from the substrate. Significant efforts have been made to mimic these adhesive systems, typically through the moulding of many “posts” in higher modulus elastomers.<sup>10,15-21</sup> Such mimics have shown increased peak forces, and roughness tolerance.<sup>16-22</sup>

In this work, we show how a thin, crumpled sheet of elastic material can form a new type of pressure sensitive adhesive that is largely insensitive to micro-scale surface roughness (Fig. 1). Specifically, we create ‘sticky crumpled matter’ by crumpling up sheets of polydimethylsiloxane (PDMS) and then we measure force-displacement curves to characterize their adhesive performance. We test against various ideally rough substrates and find that crumples have similar adhesive performance in all cases. Inspired by the results with elastic PDMS sheets, we go on to show how crumpled elasto-plastic sheets (polycarbonate coated with an adhesive layer) can be used to mimic the flow of a curable structural adhesive and amplify the overall adhesive strength to practical levels.

To understand the strength of an adhesive on a broad concep-

<sup>a</sup> Materials and Nanotechnology, North Dakota State University, Fargo, USA.

<sup>b</sup> Department of Physics, North Dakota State University, Fargo, USA. Tel: +1-413-320-3810; E-mail: andrew.croll@ndsu.edu

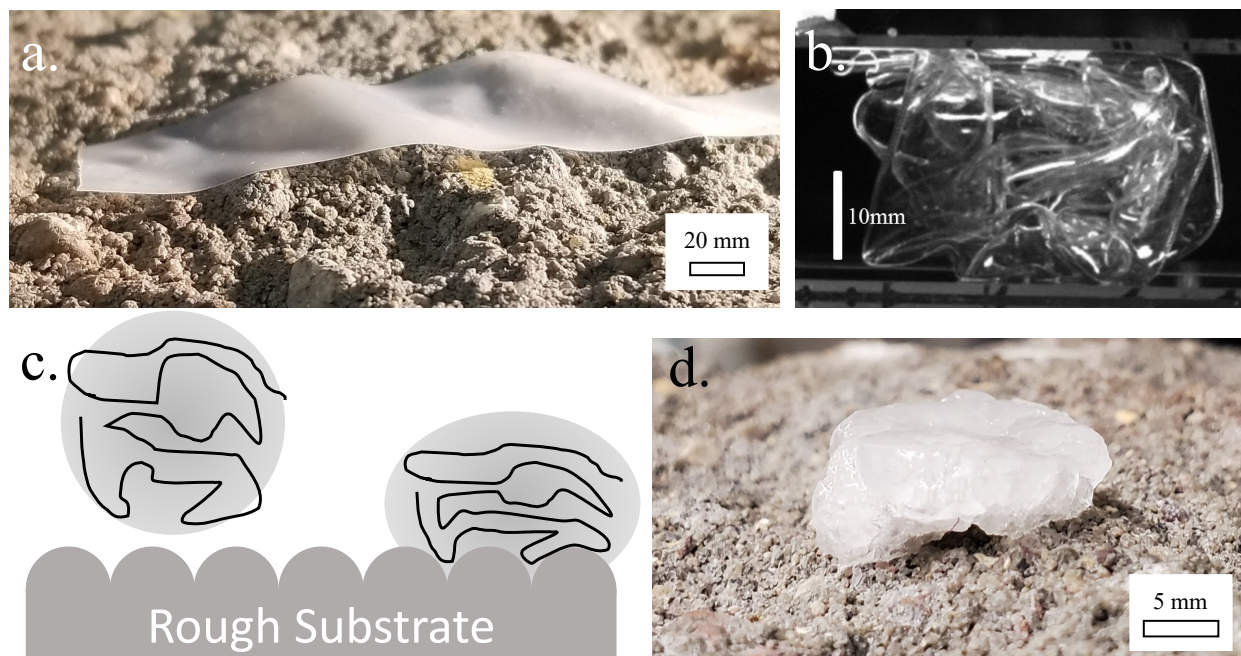


Fig. 1 Temporary adhesion on rough surfaces. a.) A piece of tape on a rough substrate. The tape makes little true contact and does not stick well. b.) A sticky crumple between two parallel glass plates, showing the complex internal structure. c.) Schematic of a cross-section of a crumpled sheet before and after being compressed into a rough substrate highlighting how the deformation increases surface contact. d.) A polycarbonate crumple adhering to a rough substrate after an experiment. In this case, the interface failed on the flat steel plate rather than the rough brick substrate. Note that the crumple remains flattened due to plasticity and adhesion in the crumple.

tual level, it is useful to reduce the system to the contact between an adhesive continuum solid and another substrate continuum solid. The system's overall free energy can then be modeled as it responds to an applied force.<sup>23–25</sup> A very simplified fracture-mechanics approach leads to a scaling prediction of the peak force held by an adhesive before it is separated from a surface:

$$F \sim \sqrt{\frac{G_c A}{C}}, \quad (1)$$

where  $G_c$  is the critical energy release rate,  $A$  is the contact area and  $C$  is the system's compliance.  $G_c$  is a materials property of the adhesive interface similar to a work of adhesion, and so characterizes the interfacial chemistry. The compliance is defined as the derivative of the indentation depth,  $x$ , with respect to the applied force  $F$ , and characterizes the softness of the adhesive.

Strictly speaking, Eqn. 1 only applies in the case of a purely elastic material and a contact which fails unstably. While not universal, Eqn. 1 clarifies the main challenges of adhesive design for rough surfaces: the need to maximize  $G_c$  and  $A$  while minimizing  $C$ . If the adhesive does not change states as a structural adhesive might, then roughness will lead to low contact area unless compliance is high. The catch-22 is that high compliance also leads to low peak forces held by the adhesive. Luckily, adhesives need not be solid continua as can be seen in the biological world.

Rather than creating complicated moulded topographies to mimic biology, we choose to exploit the naturally hierarchical structure created when a thin sheet is subjected to 3-dimensional confinement.<sup>26–29</sup> The mechanics of a crumpled sheet are now well explored in the literature<sup>26–39</sup>, though considerable theoretical

debate about the origins of the structure continues.<sup>30,34,36,38</sup> A recent practical advance has been the establishment of a simple, empirical, scaling rule for describing the compressive load held by a crumpled ball.<sup>34,35,37</sup> If a crumpled ball is compressed between two parallel plates, the force,  $F_{cm}$  is related to the plate separation  $H$  as:

$$F_{cm} = \bar{E} t^2 (2R/H)^\alpha, \quad (2)$$

where  $\bar{E}$  is the plane strain modulus of the sheet,  $t$  is its thickness,  $R$  the radius of the crumpled ball and  $\alpha$  is an exponent. Experimentally, the exponent is known to vary from material to material, but does seem to have well defined average values.<sup>30–33,37</sup> Note that this implies a very non-linear compliance for a crumple, in particular  $C = H^{\alpha+1} / (\alpha \bar{E} t^2 (2R)^\alpha)$ , which means a crumpled adhesive would be expected to be pressure sensitive.

Our basic hypothesis is that a thin sheet, when crumpled, forms a roughness tolerant PSA-like adhesive. In other words, the crumpled adhesive will produce high losses during pull off, the losses will be caused by viscoelastic processes as parts of the sheet peel, the peak force will be relatively low, and all this will occur in the same way when the adhesive is attached to a long-wavelength rough surface as when it is attached to a smooth surface. This notion is based on the idea that the crumpled material is hierarchical so can deform around large scale roughness, and that a crumpled sheet is still a sheet so will peel at multiple contact points (both internal and external) when removed from a surface. Further advantages of crumpled materials include an ability to tune the peak adhesive force through the mechanics of the crumpled state, as previous work suggests that a crumple increase its compliance under increased pressure. A final advantage is that

different materials can be easily crumpled which can lead a strategy of optimization for various applications. We therefore begin our investigation by examining sticky crumpled sheet from the perspective of a PSA in the absence of roughness. We then show how a single cylindrical obstacle does not significantly alter the adhesion in any observable sense. We go on to explore several idealized rough substrates, comparing the behaviour of crumpled adhesives and solid blocks of identical materials. Finally, we show how the elastic sheet can be switched with a plastic sheet in order to maximize the adhesive forces of the crumpled adhesive system.

## 2 Materials and Methods

### 2.1 Polydimethylsiloxane Crumples

Crumples were made of polydimethylsiloxane (PDMS) elastomers which are commonly used “dry” adhesives and are prevalent in research. PDMS also has the advantage of ease of fabrication and easily adjustable mechanical properties. In this case, PDMS sheets were made through mixing a desired weight ratio of Sylgard 184 elastomer base with Sylgard 184 curing agent. Ratios examined were 10, 15, 30, 40, 45, and 50 parts elastomer base to one part curing agent.

The Sylgard 184 solution was thoroughly mixed for  $\sim 10$  min and then placed on a substrate through dropcasting, flowcoating, or spincoating; the specific method used depended on desired thickness. Once Sylgard 184 solution was spread evenly on a substrate the sample was placed into a vacuum oven set at  $\sim 760$  Torr for cycles of 5 minutes until bubbles no longer appeared. Annealing was carried out in vacuum oven at a temperature of  $85^\circ\text{C}$  and a pressure of 380 Torr for a duration of 90 min. Samples were quenched by removal from the oven then were allowed to cool fully prior to experimentation.

Sheets were cut into squares or rectangles and separated from their substrate. The dimensions of length and width of sheets were measured via calipers prior to experiment while thickness was measured from sheet remnants on substrate or after experiment using confocal microscopy. Thickness in samples was only measured after experiments in order to preserve the integrity of the sample. This is because calipers have sharp edges which could conceivably damage a sample and the added preparation for microscopy could cause dust to adhere to the sheet.

### 2.2 Polycarbonate Crumples

Solutions of 60 kg/mol molecular weight Polycarbonate (PC) and chloroform were mixed in ratios of 1-10 % by weight. PC was used as received from Scientific Polymer Products, and chloroform was used as received from Fisher Scientific (Optima grade). Solutions were allowed to mix for 48 to 96 hours prior to use in order to ensure complete dispersal of polymer in the solvent. Solutions were then drop cast on freshly cleaved mica substrates. Mica was held by capillary force from a drop of water to a glass slide for support and stability. Samples were then immersed in a chloroform vapor environment in order to slow down the evaporation rate. Samples were left in these chambers for at least 12 hours prior to annealing at approximately 180 degrees on a hot stage. The annealing step drove off any residual solvent, reduced

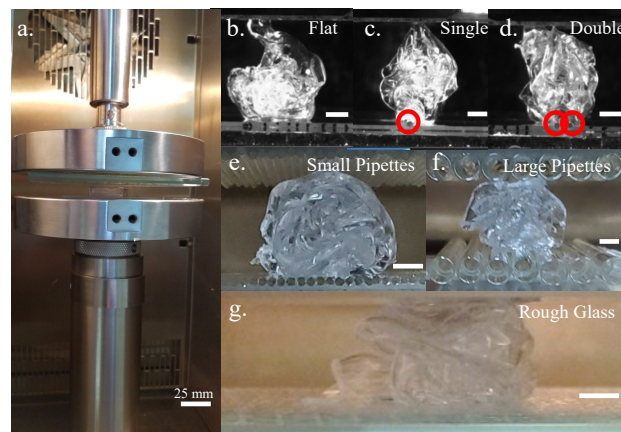


Fig. 2 Experimental details. a.) Instron with glass plates and a “Bulk” sample. b.) Close up of a flat glass/ crumple experiment. c.) A single capillary tube/ crumple/ flat glass experiment. The single capillary tube is highlighted with the red circle. d.) Two capillary tube/crumple/flat glass experiment. Capillaries are highlighted with red circles. e.) A symmetric many capillary tube experiment. f.) A symmetric large pipettes experiment. g.) A rough glass/crumple/flat glass experiment. Scale bars indicate 5 mm unless otherwise noted.

any stress from the evaporation process while also allowing the surfaces to become more smooth.

To create greater adhesion, an adhesive layer was applied to both sides of the PC sheet. This was done as follows. First, a glass slide was spin-coated with a thin layer of polyacrylic acid (PAA). This serves as a water-soluble release layer. Then Dow-Corning MG-2402 Silicon Adhesive was spin coated on the PAA layer. Next, the annealed polycarbonate sheet was released from its mica support through the use of a water drop. It was lifted from the mica via tweezers, and allowed to dry in ambient conditions. The sheet was then slowly laminated to the adhesive layer in a manner resembling a peel experiment, though in reverse. Finally, the sample was placed on the spin-coater and a second layer of adhesive was spin cast on top of the PC.

Samples were allowed to dry over several days and were then cut to size with a scalpel, and removed with addition of water. sheets were extremely sticky and crumpling was challenging, though most samples could be eventually crumpled to a similar density as an unmodified polycarbonate sheet.

### 2.3 Comments on Crumpling

In our work we emphasize the randomness of the crumple structure, rather than try to control it. In other words, we make no effort to create a well defined process to create a crumpled sheets. Here, sheets were crumpled by (gloved) hand until a desired, roughly spherical, shape of a particular radius was reached. At this point the crumple would be placed between the plates of the test apparatus, as in Fig.2a. Crumples were always created by at least two different people, on many different days, and with several materials as outlined above.

In this work, we also opted to reduce the incredibly large parameter space by focusing on crumples of an approximately fixed radius and sheet thickness. Earlier work has focused on how these

variables affect the compression part of the cycle, and we felt that repeating this work would only distract from our main message: crumples are a PSA-like adhesive that is roughness tolerant. We imagine that at other densities the adhesion forces will affect outcomes, but away from extreme limits (density approaching zero or approaching a solid material) the behaviour will be qualitatively similar to what is discussed here. A future work may characterize these details.

## 2.4 Rough Substrates

Idealized roughness was introduced to plates in order to test the crumples effectiveness in adhering to rough surfaces. Kimble Chase Geresheimer borosilicate glass capillary tube(s) with an outer diameter of 1.7 mm were glued onto a glass plate. The glass capillary tubes create a simple, chemically identical obstacle to investigate. Several variations were investigated. First a single capillary tube was glued to a glass plate such that the glue (epoxy) was outside of the intended contact area in order to maintain a pure glass surface. Next, two tubes were glued to the substrate such that they were spaced out by a tube diameter. Finally, many capillary tubes were arranged along the substrate (see Fig. 2). In this final case we report the power spectral density in figure 3 as it is the most comprehensive measurement of roughness available to us. Measurements were conducted with a KLA Tencor P-15 Profilometer with a tip radius of  $\sim .25 \mu\text{m}$ . While an inferior measure, we also report the RMS roughness of  $1.7 \times 10^{-3} \text{ m}$  for completeness. The power spectral density of the flat glass used is also displayed in Fig. 3 for comparison (RMS roughness of  $6.3 \times 10^{-6} \text{ m}$ )

Glass pipettes of outer diameter 6.86 mm were also used as a model rough substrate. In this case many pipettes were packed tightly against one another and glued to a glass plate. RMS roughness was calculated to be  $8.4 \times 10^{-4} \text{ m}$ . In this case the power spectral density was measured with a fluoview 1000 confocal microscope using a 543 nm laser and a pixel size of  $1.263 \mu\text{m}$ . Several images were stitched together to increase the measurement range over the size of one pipette diameter, though the field of view could not resolve the contact point between two adjacent pipettes (it is beyond the working distance of the lens used). This means the RMS value is not completely accurate, but serves as an approximate value in this case.

A rough glass plate, “504 Rough Cast - textured architectural glass”, was donated by Bendheim and used after cleaning with acetone. The plate has a roughness which is characterized by the power spectrum shown in Fig. 3. In this case only flat plate/crumple/rough glass plate experiments were conducted. RMS roughness was calculated to be  $1.6 \times 10^{-4} \text{ m}$ .

A landscape brick was obtained from a local hardware store. Its chemical make-up is unknown, but the brick was primarily made of cement, sand, and gravel. The roughness of the brick is also shown in figure 3. RMS roughness of the brick is  $3.1 \times 10^{-4} \text{ m}$ .

## 2.5 Crumple Compression Experiment

Several apparatus were used depending on the scale of forces present. First, a microscopic setup was used. In this case a Physik

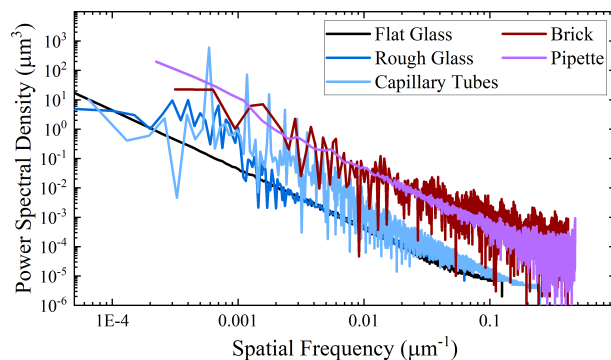


Fig. 3 Power spectral density of rough substrates. Roughness of substrates was characterized via profilometer or confocal microscopy. Flat glass shows a power law of approximately  $-2$ , and the capillary glass sample shows peaks at 1.7 mm as expected. The rough glass shows a broad set of peaks in the same low frequency range. Glass pipettes were too large in aspect ratio for the profilometer, so were measured with the confocal microscope. Pipettes still appear relatively flat with the observed range ( $\sim 1 \text{ mm}$ ). The brick was also too large for the profilometer and its roughness was also measured with the confocal microscope.

Instrumente N-381.3a actuator moved a glass plate and a parallel plate was mounted to a Transducer Technologies force transducer. This whole setup could fit under a confocal microscope to aid observation. A second setup used a lab camera and telescope to observe a NI motor move a plate while a parallel plate was mounted to a Denver Instruments lab scale for force measurement. Finally, the most commonly used apparatus involved an Instron 3400 universal test machine to move plates and measure forces. Here double sided tape was used to mount the various glass plates tested.

Sheets were compressed by gloved hand from the outside in until a roughly spherical crumpled ball was formed. The exact internal structure composition of each crumple sample was random and unique. The crumple was then placed between clean glass slides at minimal compression for sufficient contact to be established. Compression was then carried out with one plate stationary while the other moved by actuating motor at a set speed to a set displacement (5 mm/min unless otherwise specified). Note that motor speed will affect the energy release rate during adhesive separation, particularly for elastomers and traditional PSA's. We choose to fix speed in order to focus on the main message of roughness tolerance. The motor then moved the movable plate in the opposite direction to a point past the starting point for complete separation of the crumple from one of the plates. Force and distance measurements were taken throughout the compression-retraction cycle. Crumple samples were tested at least three times in succession varying the location of the rough plate. We also note, that many individual sheets are used in our testing. Each crumple is unique, so the average behaviour is necessary for a reproducible understanding of behaviour.

## 3 Results and Discussion

### 3.1 Smooth Plates

Figure 4 shows a typical compression and retraction cycle for a crumpled PDMS sheet. The crumple starts at some small, nonzero

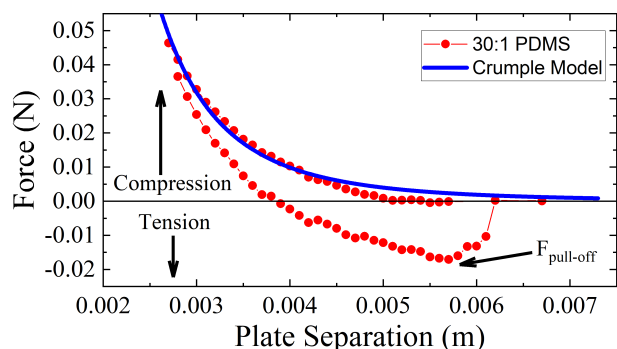


Fig. 4 Typical data from a smooth plate compression experiment. Here a 30:1 PDMS sample of dimensions  $44.3$  by  $43.9$  by  $2.32 \times 10^{-2}$  mm is crumpled to a radius of  $12.2$  mm. The indentation portion of the curve is fit with a power-law which results in an amplitude of  $F_0$  of  $1.91 \times 10^{-12}$  Nm $^\alpha$  and  $\alpha$  of  $4.06$ .

force as it requires some load simply to maintain its confinement between the two glass plates. When no load or confinement is applied to a crumple they tended to undergo dynamic rearrangements and opening, especially in cases of higher modulus, lower adhesion, and thicker sheets. As the plates are compressed the force rises following a power-law,  $F = F_0 H^{-\alpha}$ , as shown by the solid line in Fig 4. The power law is generic;  $F_0$  is an amplitude,  $\alpha$  is an exponent both determined by fitting the data with  $H$  is the plate separation. We make no analysis of this as the power-law shape is well-established in the literature.<sup>30,34,37,39</sup> More important to this work is that the force increases monotonically to some maximum force obtained at a predetermined plate separation (a fixed displacement). As the motor is reversed and the plates are separated the forces dropped quickly to zero and then typically fall below zero and reach a peak tensile force (a minimum in the force curve). In figure 4 a peak tensile force ( $F_{pull-off}$ ) is marked with an arrow and in this case has a value of  $0.017$ N (we drop the negative sign to simplify discussion). After the minimum, the tensile force decreases in magnitude (becomes less negative) and ultimately drops to zero after pull off. The compression cycle shown in Fig. 4 is hysteretic, indicating an energy loss in the cycle.<sup>39</sup>

The rise in forces back to zero does not necessarily follow the same curve shape in every experiment. Curves can have a smooth, well-defined tensile peak (as in Fig. 4), an elongated plateau, or decreases in tension that appear as steps as certain parts of the crumple open (see Fig. 6 below). In this way, the hysteresis of the crumple differs notably from that of simpler thin sticky sheet systems such as a tape loop which reaches a tension plateau during pull-off.<sup>40</sup> Crumples are dynamic, complex shapes which tend to shift during retraction as the confinement is decreased, and internal rearrangements become possible. The differences in pull-off curves observed here are due, in part, to the randomness of the structure and cannot be avoided. In short, statistical or average behavior must be considered.

More generally, we find stiffer, lower  $G_c$  crumples to fail with a well defined pull-off force (as in Fig. 4). When failure occurred with a well defined peak it appeared that the contact line moved

much as in a solid sphere (JKR) experiment - proceeding more or less uniformly from the outside edge of the contact zone towards the center of the crumpled sheet. Even in this case, variation was occasionally noted and longer plateaus could form during pull-off.

Typically a plateau in tensile force would occur if the crumple unraveled under tension as unraveling often lead to moments of stable peel either internally, or against the glass substrates. As sheets were made softer or stickier, unraveling was much more likely during pull-off because more of the crumples are flattened against the smooth plates. The increased contact requires larger forces to pull off at once, so any location with a small amount of asymmetry will peel in one direction first. This second type of failure is notably similar to a PSA tack curve. In the case of a PSA, the plateau is typically related to the growth of voids created through a cavitation process occurring under the high stress of the tensile peak.<sup>41-43</sup> The crumple starts with many voids, so it is not surprising that under certain conditions these can grow in a similar manner to cavities in a PSA.

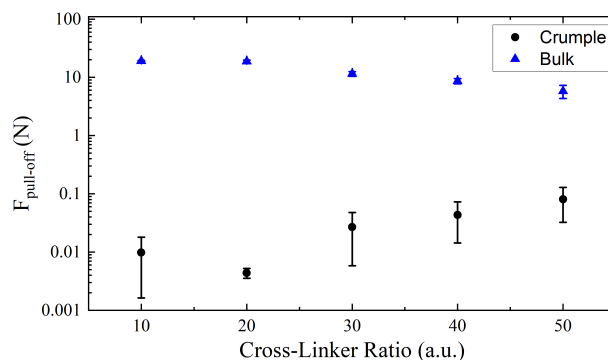


Fig. 5 Average pull-off forces (peak tensile forces) for different crosslinker ratio PDMS crumples and bulk samples. As cross-link density decreases, the prevailing trend is towards increasing forces. Note that the 10 to 1 ratio measurements include several experiments in which zero force was measured, whereas other cross-link ratios always measured non-zero values of peak force. Error bars from standard deviation of repeated measurements new crumpled sheets. Measurements were conducted on  $N$  new sheets where  $N$  was 4 for 20 to 1, 9 for 30 to 1 and was greater than 10 for the other samples.

We next consider the magnitude of the peak tensile forces, or more simply the pull-off force ( $F_{pull-off}$ ). Here thicknesses varied slightly from sample to sample (each was measured individually, but were held in the  $500 \mu\text{m}$  range to simplify comparison (standard deviation about  $80 \mu\text{m}$ ). Likewise, sheet size was held at approximately  $5.5 \times 5.5$  cm. When crumpled, the average radius was approximately  $1.3 \pm 0.5$  cm. In these experiments the motor speed was fixed at  $0.085$  mm/s. Under these controlled conditions a rational comparison between pull-off forces of the different PDMS ratios could be made. The basic result is shown in figure 5. Forces are observed to rise as the cross-link density falls, similar to what is observed in a Johnson-Kendal-Roberts spherical probe test. Here we see the opposite trend with bulk (unstructured rectangular prisms) PDMS because the pull-off force in this geometry incorporates both  $G_c$  and  $E$  which both change with crosslinking in PDMS.<sup>23,40,44</sup> Crumples have much lower adhe-

sion forces than bulk samples, similar to what is seen with typical PSAs.

The measured pull-off forces with crumples are not far from what one would estimate for a sphere of similar material (a JKR test). For example, a sphere of 30 to 1 PDMS of radius 1.5 cm and  $G_c$  of 0.64 N/m would pull off at a tensile force of about 0.045 N, assuming a JKR model (i.e. that  $F = (3/2)G_c\pi R$ ). The average measured value for 30 to 1 crumples is 0.024 N. The reduction in force is likely due to the reduced contact observed with a crumpled sheet (discussed further below).

Overall cycle hysteresis was also found to vary, increasing with decreasing cross-link density. A detailed analysis of the effect is discussed in<sup>39</sup> and as the hysteresis is not important to our discussion of roughness tolerance it will not be considered further. Additionally, because of the low pull-off force measured for 10 to 1 and 20 to 1 samples, these cross-link ratio sheets will not be used further in tests of roughness tolerance.

### 3.2 Interaction with an Obstacle

After baseline experiments with crumpled PDMS sheets between flat plates we consider the behaviour when a simple obstacle is in the contact zone. Specifically, we examine adhesion of a crumple in the presence of a single cylindrical glass capillary tube, or two spaced apart cylindrical glass capillary tubes. The obstacles were alternated between the top and bottom plates of our setups in order to study any influence of gravity on the experiments. Additionally, the order of the experiments were randomized in order to minimize any systematic effects of fatigue or contamination. Glass was cleaned between experiments with an acetone soaked kimwipe. Typical results can be seen in Fig. 6.

The experiments were run with the 3 stickiest PDMS ratios, but all produced similar outcomes (though with differing pull-off forces). In short, there was no discernible difference in force curves between samples on smooth or obstacle laden surfaces. Figure 7 shows three typical experiments with a 50 to 1 sheet, where all experiments shown were picked because they detached from the top (smooth glass). When we analyse the pull-off forces in detail, we again see no statistically relevant difference between smooth plates and plates with one or two obstacles. For example, with 40 to 1 crumples we find smooth plates in these experiments to hold a force of  $0.037 \pm .02$  N, one obstacle is  $.046 \pm .03$  N and two obstacles had an average of  $.041 \pm .04$ .

The presence of obstacles did not dictate which side (top or bottom plate) would start to debond first, or which side would debond fully at the end of the experiment. Crumples were more likely to remain on the bottom plate (65 % of experiments), but no difference in pull-off forces were noted either type of separation. If a sheet were to remain on the top plate, its weight was subtracted from the raw peak force in order to account for the change in zero. Which plate the crumple was first attached to before compression also did not dictate which plate the sheet would remain attached to at the end of a cycle.

In most adhesive geometries contact area influences the pull-off force, with larger contact areas leading to larger forces. When an obstacle or roughness is placed in between an adhesive and a

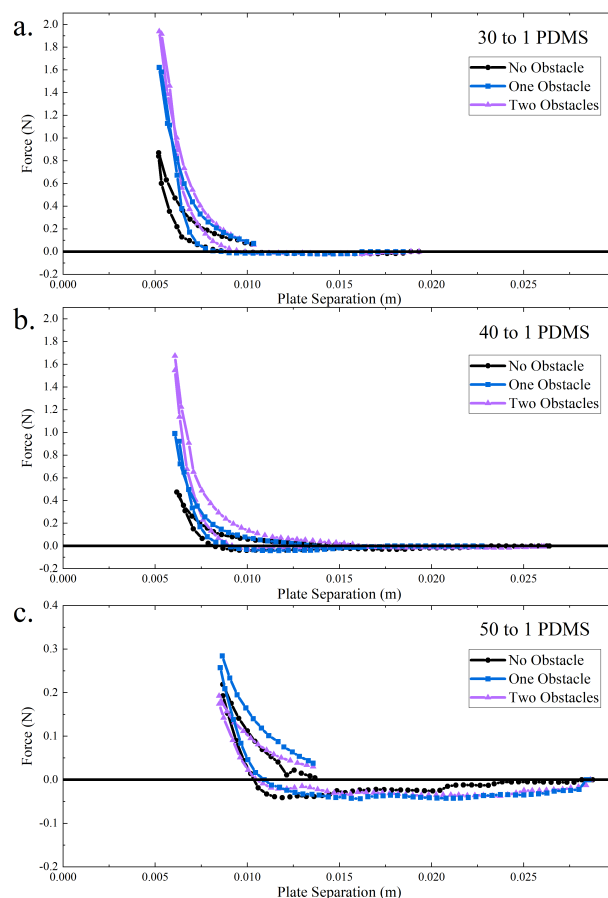


Fig. 6 Experiments with an obstacle. a.) 30 to 1 PDMS crumpled sheets interacting with flat glass (black circle), one capillary tube (blue square) or two capillary tubes (light blue triangles). There is no discernible difference in pull off forces. b.) 40 to 1 PDMS crumples undergoing the same obstacle tests. Again, no statistical difference is noted between pull-off values. c.) Similar tests for 50 to 1 PDMS, in this case the indentation pressure is decreased to show the pull-off more clearly. Again, no differences are noted.

substrate it is commonly understood that contact area will be reduced.<sup>45,46</sup> In the case of crumples, because forces do not change, it seems that the contact area must also remain unchanged.

Figure 8 shows a series of experiments in which we directly monitor the contact area between a 40 to 1 ratio PDMS sheet and a smooth or single obstacle substrate. Figures 8a. and e. show a fluorescence image of the crumple below a smooth plate, and the same crumple below a single obstacle surface (the black line up the center is the non-fluorescent obstacle). Figures b.-d. and f.-h. show a series of images of the glass surface take at increasing compression. These images are unfortunately complicated by the interference created by the illuminating laser and the glass plate. In our sample cell the top plate is fixed and tilt/yaw control is located below the bottom plate. Plates are made parallel to one another, but we cannot make them parallel to the optical axis at the same time. Regardless, contacting domains show up as grey regions and can be observed and carefully measured by hand. Both experiments show patchy irregular contact areas which bring to mind the contact splitting seen in organisms such

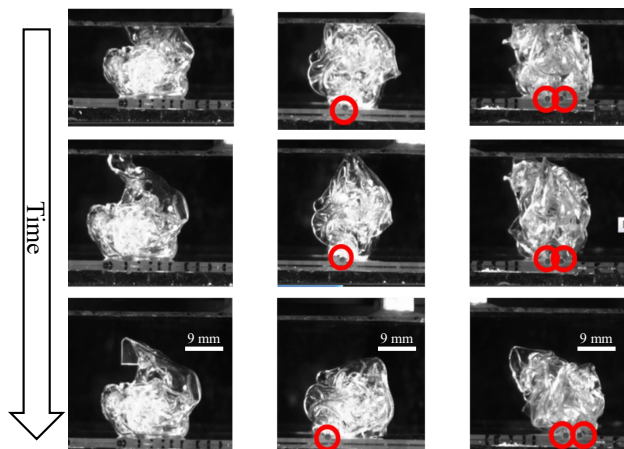


Fig. 7 PDMS experiments at different points of the retraction cycle. Note how there is not much difference in the separation and all remained on the bottom plate even for samples with roughness. All three experiments used the same 50 to 1 PDMS sheet with dimensions of 0.48 mm thickness, 54 mm length, and 54 mm width, the average radius of the crumples was 12 mm, 10 mm, and 13 mm, respectively.

as lizards and insects.<sup>13,14</sup> Contact splitting is a set of beneficial effects found in fibrillary and other multiply broken contact adhesives and is thought to help organisms manage adhesion to rough substrates<sup>18</sup>. The patchy contact area with a crumpled adhesive is not surprising due to the hierarchical structures of a crumple.<sup>26</sup> The Broken contact also resembles the complex fingering and cavitation observed in some PSA's during detachment.

Figure 8i. shows the force curves from the two experiments, which overlap almost perfectly, indicating that the crumple structure is largely unchanged between the two experiments. Figure 8j. shows the measured contact area for both experiments as a function of overall compression. The two curves show an almost identical trend, though the obstacle sample shows slightly reduced contact area. We believe that this is due to measurement; the amount of contact between the obstacle and the crumple cannot be resolved or measured directly but is clearly non-zero. In short, due to the complexity of the crumple structure the crumpled adhesive simply deforms around the obstacle with little or no change in elastic energy.

### 3.3 Model Roughness Experiments

The success of the crumpled adhesive in tolerating the presence of obstacles warrants further exploration with more complex and realistic rough surfaces. In order to maintain chemical simplicity, glass was used to create three ideally rough substrates. The first substrate is made of many glass capillary tubes packed closely together (rather than the one or two used previously). The second is made of many pipettes packed closely together. The final is a textured glass plate. The lateral scale of the roughness used scales a range of sizes from about the crumple radius (about 1.5 cm), roughly half this size, and roughly a tenth of the crumple radius. This in addition to the nominally flat glass plates. To highlight the unique behaviour of the crumpled adhesives we compare crumple results with those of solid rectangular prisms of PDMS with dimensions 29 by 29 by 7.5 mm (which we refer to as bulk sam-

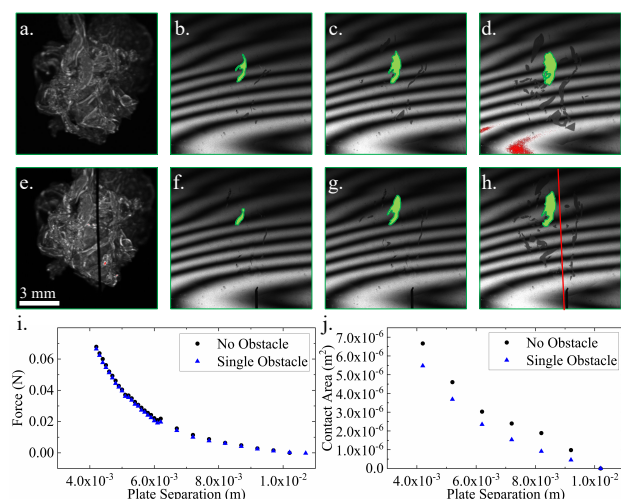


Fig. 8 Evolution of contact area. a.) Fluorescence image of a crumpled 40 by 40 mm, thickness 57  $\mu\text{m}$ , 40 to 1 PDMS sheet between two parallel glass plates. b.) Image of contacting glass surface illuminated with a laser. Unfortunately the laser illumination leads to interference which makes it difficult to see the small patches of contact between the smooth glass plate and the PDMS crumple. c.),d.) Increasing compression leads to increasing contact area. e.) Fluorescence image of a second experiment in which an obstacle has been added (vertical black line due to lack of fluorescence). f.) Image of glass surface, showing contacting patches of PDMS. g.),h.) Increasing compression once again leads to increasing surface contact. Red line in h. indicates the position of the obstacle. All images are identical in size. i.) Force displacement data for both experiments, showing almost identical curves. j.) Contact area as a function of displacement for both experiments. Obstacle experiment shows slightly lower contact area, which is likely due to the contact between the obstacle and sheet not being imaged.

ples). The results of these experiments are shown in figure 9.

The bulk samples (solid rectangular prisms, Fig. 9a.) show moderate levels of adhesion (pull-off force), though adhesion levels vary with the various substrates. All show failure without any significant plateau, indicative of a simple interfacial failure (e.g. no cavitation). In this particular experiment, the rough glass substrate has the largest adhesion value, though this varies from experiment to experiment and depends on the elastomer modulus and applied compressive force used in the experiment (see Fig. 10 below). In the case of soft elastomers, the long wavelength, low amplitude roughness of the textured glass can lead to increased contact area when compared to a flat glass plate, which explains why its peak force is greater than that of the flat glass plates.<sup>45,47</sup> The effect also contributes to the effective stiffness of the system (slopes in Fig. 9a.); the rough glass experiment shows the highest stiffness because additional elastic energy is stored in the deformed interface.

The large lengthscale roughness of the pipettes shows the lowest overall adhesion, even with additional compression. Again, this is a result of changing contact area. The bulk PDMS sample cannot deform enough to come into complete contact. This also shows in the low slope of the curve, little contact means much of the elastomer is unstressed during indentation. The average results from all substrates are summarized in figure 9c. where the ratio of peak force on substrate  $X$  to peak force on flat glass is

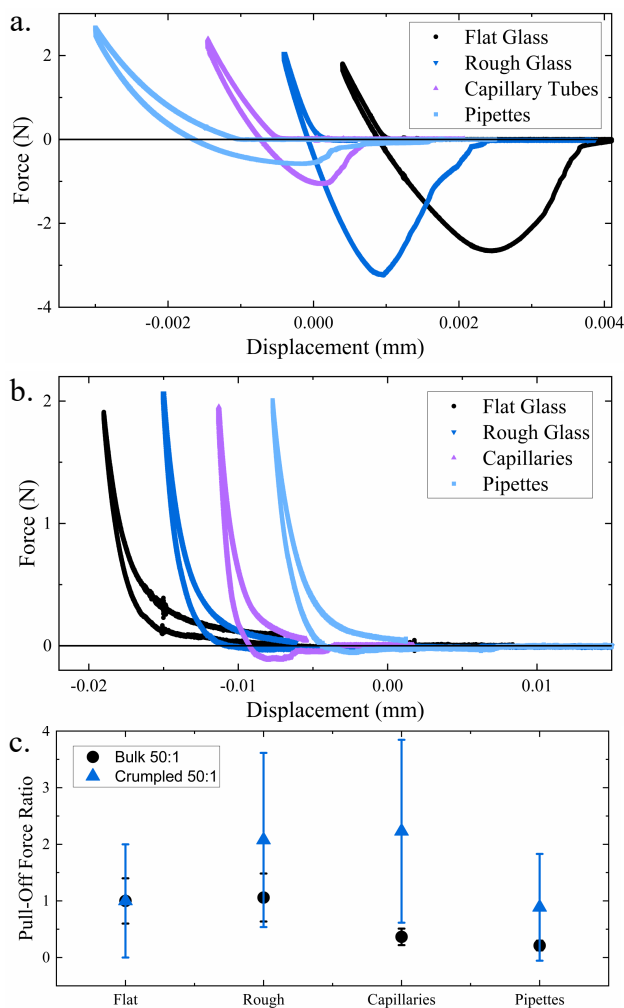


Fig. 9 Roughness performance of crumpled adhesives. a.) Bulk samples of 50 to 1 PDMS (29 by 29 by 7.5 mm prisms) tested on various substrates. Adhesion is moderate, but is reduced on rough substrates. b.) Similar experiments conducted with a 70 by 70 by 0.82 mm crumpled 50 to 1 PDMS sheet (average diameter in the crumpled state 30 mm). Adhesion is reduced, but remains similar on all substrates. Note the data in a. and b. are off-set arbitrarily along the displacement axis for clarity. c.) Ratio of average peak force on substrate  $X$  to average peak force on glass for the bulk samples and for the crumpled samples. Error bars are from the standard deviation of the measurements

plotted.

Figure. 9b. shows the basic outcome for crumpled sheets interacting with rough substrates. Peak forces are once again found to be low compared to bulk samples, and little variation is observed between the peak forces recorded on different rough substrates. The effective stiffness of each, while non-linear, appears to be almost identical on each substrate. This suggests again that the true contact is similar in each experiment, though it could not be measured directly due to the complexity of imaging through rough substrates. Finally, we note that the crumpled sheets required much larger distances to fully break contact because internal interfaces are also opening during the pull-off process and dissipating energy. The solid elastomer behaves as an ordinary continuum, but the crumpled elastomer now appears more simi-

lar to a pressure sensitive adhesive.

The average behaviour, summarized by a ratio of peak force of a crumpled adhesive on substrate  $X$  to peak force of a crumpled adhesive on a flat substrate, is shown in Figure. 9c. The data shows that on the rough glass and the small capillary substrates the crumples perform significantly better than on flat substrates. Once again, the weakest performance was observed with the large capillary tubes, where the crumples also show a relative decrease in functionality to similar levels as the flat substrates (though not as severe as with the bulk samples which are worse than flat glass). The increased performance on rough substrates shows that the effect is not limited by the horizontal scale of the roughness in this range. As the capillary tube substrates are about a tenth of the crumple radius, we conclude that any limiting roughness scale must be below this size. As the crumple is a statistical object, and will have facets (or pores) of many different sizes between the crumple radius and the sheet thickness, it seems that facets are not a limiting substructure. We hypothesize that the effect will only be limited at roughness scales comparable to the sheet thickness, as the sheet could no longer fit between obstacles spaced more closely than the sheets thickness.

The data shown in Fig. 9a. and b. was collected at similar peak normal forces because peak normal force is well known to affect adhesive performance on rough substrates.<sup>6,45,47-50</sup> Fig. 10 shows the peak adhesive force recorded for all substrates and samples at a variety of different peak normal forces. Unsurprisingly, bulk samples on flat substrates show little variation with increasing normal force. This is because the elastomer is soft enough that the van der Waals interactions easily pull it into intimate contact after which additional pressure simply cannot increase contact.

Bulk samples on the rough glass show a considerable change in peak adhesive force with low normal forces, but reaches a plateau at a normal force of about 1 N. On the rough glass, van der Waals forces are not large enough to pull the sample into full contact so additional normal force can increase overall contact.<sup>45,48,50-52</sup> At some point contact does become complete, and additional normal forces do not increase the adhesive force any further. If the intrinsic adhesion is great enough to stop the elasticity of the interface from deforming back to flat when the normal force is removed, an increase in adhesion results from the increased contact area.<sup>47</sup> The other two rough samples (pipettes and capillary tubes) also show increasing adhesion with increasing normal force but never reach a plateau. In this case, the material is not able to deform all the way into the crevasses formed between the glass cylinders. Forces remain lower than the flat glass because contact area remains decreased from the  $\sim 100\%$  achieved with flat glass contact.

The crumpled adhesives show considerably more scatter but show no clear trend with increasing normal force. This is true regardless of the substrate or its roughness, again showing how insensitive to roughness the crumpled adhesive is. As the crumple contacts a surface, van der Waals forces allow a certain amount of the crumple to make contact with the surface regardless of the surface roughness. However, in the PDMS system, additional deformation is simply stored elastically and released when the

driving normal force is removed. That the peak adhesive force is independent of the normal force considerably simplifies adhesive design, but the low values limit the application of PDMS crumples.

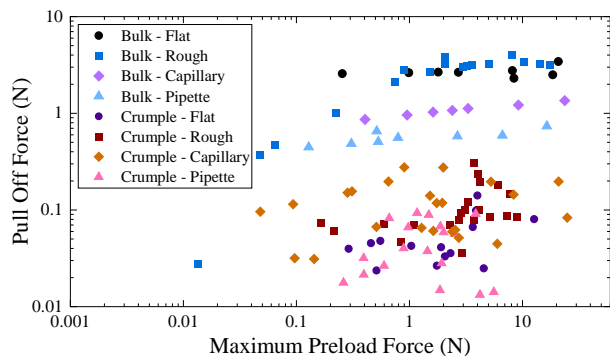


Fig. 10 Pull-off force,  $F_{pull-off}$ , as a function of peak normal force. Bulk samples are 29 by 29 by 7.5 mm pieces of 50 to 1 PDMS and crumpled samples are 70 by 70 by 0.82 mm samples crumpled to an average radius of 30 mm.

### 3.4 Increasing Pull-Off Forces

Crumpled PDMS adhesives tolerate roughness well, however, they do not achieve large peak forces. The low pull-off forces are a result of low contact area combined with the low modulus of the PDMS used.<sup>25</sup> Typically, low contact area is combated by reducing the stiffness of the adhesive in order to create more deformation and surface contact. Unfortunately, reducing an adhesive system's stiffness also reduces its peak adhesive force in most geometries. What is needed to increase the adhesive force is a material which is stiff, but at the same time can deform into a high degree of contact.

Many organisms that rely on adhesion to rough surfaces for survival have evolved structures which are rigid, but thin.<sup>7,8</sup> Thin structures can easily bend around roughness, but are rigid when loaded along their length. In other words, stretching is much more energetically costly than bending in slender structures. This concept also underlies the behaviour of the crumpled adhesive which is made from a thin sheet and easily deforms around roughness given its irregular structure. However, as observed above, little adhesive benefit is gained with increasing normal force deforming the crumple into the substrate if the sheet used is highly elastic.

To increase the overall adhesive strength of the crumpled adhesive system, we make two changes to the experimental system. First, rather than an elastic material, we switch to an elastoplastic sheet.<sup>53</sup> We do this to combat the release of elastic energy after a normal force is removed by storing the deformation plastically in the crumpled sheet. We also switch to a material, PC, with a modulus roughly 5 orders of magnitude larger than the 50:1 PDMS. This increases the overall stiffness of the system, while maintaining the crumple's geometric ability to deform around roughness.

Thin PC sheets are easily fabricated, for example by spin coating polycarbonate from solution. However, micron-scale thick-

ness PC sheets will have very little adhesion upon contacting a substrate because microscale roughness will inhibit true contact (which is why organismal structures tend to be on the nanoscale).<sup>7,8</sup> To combat this flaw, we spin coat an adhesive layer (Dow-Corning MG-2402 Silicon Adhesive) on both sides of a thin PC sheet, which is then crumpled and used as described above. We also create disks of diameter 16.2 mm and thickness 128  $\mu\text{m}$ , spin coated with the same adhesive, to serve as a control "post-tack" experiment.

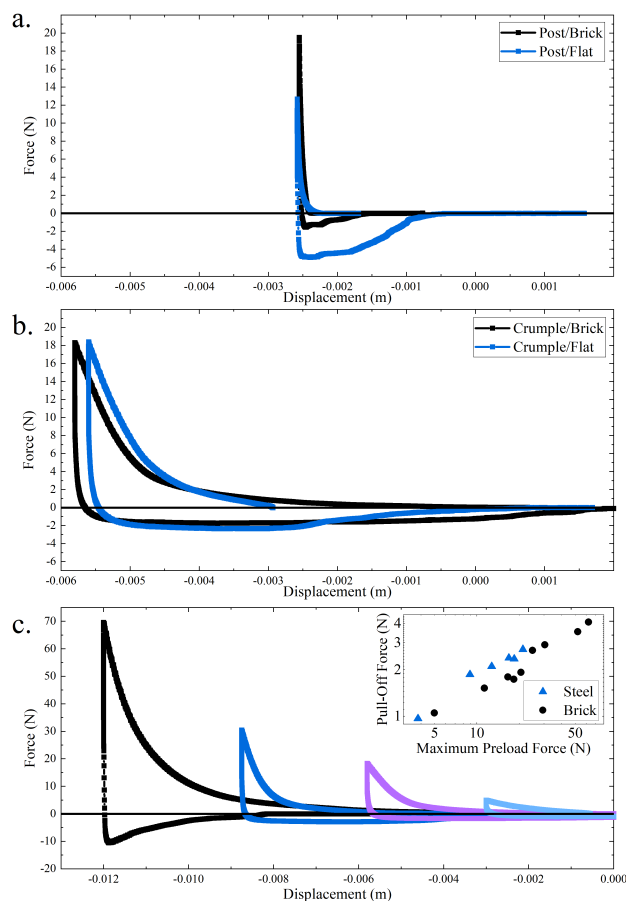


Fig. 11 Polycarbonate adhesion. a.) Control experiments using an adhesive covered polycarbonate post. Large decreases in peak adhesive force of the adhesive on the rough substrate compared to the flat substrate are evident, as is the high stiffness of the PC post. b.) Sticky crumpled PC experiments on a smooth steel substrate and a brick substrate. Samples show similar stiffnesses on both substrates and both are lower in stiffness than the post experiments. Both smooth and rough show similar peak adhesive forces which are larger than the post on brick but smaller than the post on flat steel experiments. c.) Influence of increasing peak normal force on crumpled PC adhesives on a rough brick substrate. A clear increase in peak adhesive force is seen, showing how large values are attainable with a crumpled PC adhesive. Inset shows how the peak adhesive force relates to the maximum preload force for both brick and steel substrates. Note, data has been shifted arbitrarily along the x-axis for clarity

These samples are designed to vastly increase pull-off forces, but we also expect to see a significant effect of normal forces during the compression stage due to the plasticity of the PC sheets. We change substrates in order to reach higher normal forces with-

out fracturing the cylindrical glass pipettes. This has the added benefit of relating more closely to the complex surfaces of the real world. Specifically, we use flat steel as a control surface (metals are high energy surfaces) where we would expect good adhesion for an “ordinary” PSA. We use a rough landscaping brick as a model rough surface.

Figure 11a. shows the results of the control experiments with PC posts. The post indenting a smooth stainless steel substrate shows a large stiffness upon compression, and both a large peak force and a sizable amount of dissipated energy upon pull off (e.g. a large area in the force-displacement cycle). When the post is indented into a rough brick, a high stiffness is again observed, but the pull off peak and dissipated energy are much lower.

In Fig. 11b. the force displacement cycles of a typical crumpled PC sheet is shown on the same flat steel and rough brick substrates. Both curves show decreased stiffness and both show nearly identical peak adhesive force values. Here the adhesive force is larger than the post on brick, but smaller than the post on flat steel experiments. This confirms the hypothesis that the benefits of the crumple structure observed with PDMS continue in stiffer crumpled materials (e.g. roughness insensitivity), and that the peak force can be increased with stiffer crumpled sheets.

In fact, peak forces can be increased dramatically with higher peak normal forces, as shown in Fig. 11c. This contrasts the behaviour of the elastic sheets which showed no correlation between peak force and applied normal force. The plasticity of the PC sheets keeps the structure from elastically recovering, as was intended. The peak adhesive force can also reach values of over 10 N on the rough brick, considerably higher than the post on flat steel experiment. The inset of Fig. 11c shows how the peak adhesive force relates to the maximum preload force over many experiments on steel or brick substrates. Trends show an approximately linear relationship.

## 4 Conclusion

In this work we have examined the roughness tolerance of crumpled sticky sheets. We have found that crumpled PDMS sheets adhere to surfaces, show loss during pull-off and reach low pull-off forces, similar to conventional pressure sensitive adhesives. We have also shown how crumpled adhesives deform around obstacles with little or no change to their pull-off force. This behaviour correlates with the observation of little or no change in contact area between a crumple and substrate when the obstacle is present.

Additionally, we have shown that the tolerance of single obstacles by the crumpled sheets persists when more realistic roughnesses are explored. Specifically, we show that crumpled PDMS adhesives have moderate adhesion to substrates made of flat glass, tightly packed capillary tubes, tightly packed pipettes, or long-wavelength patterned glass substrates. We also show that crumpled 50 to 1 PDMS sheets have higher peak adhesive forces on the patterned glass and the capillary tube substrates than they do on flat glass.

Noting the moderate overall peak forces of the crumpled PDMS sheets, we have developed an adhesive coated PC which was crumpled and tested against smooth steel or a rough brick. In

this case, the crumpled PC performed almost identically on the steel as it did on the brick, while measuring higher forces than a control experiment using a solid PC post and the same adhesive. Finally, we have shown how large normal forces create high peak forces on the rough brick substrate.

In conclusion, crumpling thin adhesive sheets leads to a new PSA-like adhesive system which is considerably more tolerant of substrate roughness than alternative solid body adhesives. This advance should help guide the development of next-generation roughness tolerant adhesives.

## Author Contributions

Conceptualization - ABC, Formal Analysis - ABC, TE, Funding acquisition - ABC, Investigation - TE, ABC, Methodology - TE, ABC, Supervision - ABC, Visualization - TE, ABC, Writing – original draft - TE, Writing – review & editing -TE, ABC.

## Conflicts of interest

There are no conflicts to declare.

## Acknowledgements

The authors gratefully acknowledge the support of the National Science Foundation through grant number CMMI-2011681.

## Notes and references

- 1 S. Budhe, M. Banea, S. de Barros and L. da Silva, *International Journal of Adhesion and Adhesives*, 2017, **72**, 30–42.
- 2 A. J. Kinloch, *The Journal of Adhesion*, 1979, **10**, 193–219.
- 3 A. Rudawska, *Int. J. Adhes. Adhes.*, 2014, **50**, 235–243.
- 4 S. Sun, M. Li and A. Liu, *International Journal of Adhesion and Adhesives*, 2013, **41**, 98–106.
- 5 C. Creton, *MRS Bulletin*, 2003, **28**, 434 – 439.
- 6 A. Chiche, P. Pareige and C. Creton, *C. R. Acad. Sci. Paris*, 2000, **1**, 1197–1204.
- 7 A. P. Russell, *Integrative and Comparative Biology*, 2002, **42**, 1154–1163.
- 8 E. Arzt, S. Gorb and R. Spolenak, *Proceedings of the National Academy of Sciences*, 2003, **100**, 10603–10606.
- 9 G. Huber, H. Mantz, R. Spolenak, K. Mecke, K. Jacobs, S. N. Gorb and E. Arzt, *Proceedings of the National Academy of Sciences*, 2005, **102**, 16293–16296.
- 10 C. Creton and S. Gorb, *MRS Bulletin*, 2007, **32**, 466–472.
- 11 G. Huber, S. N. Gorb, N. Hosoda, R. Spolenak and E. Arzt, *Acta Biomaterialia*, 2007, **3**, 607–610.
- 12 K. Autumn and N. Gravish, *Philosophical Transactions of the Royal Society A: Mathematical, Physical and Engineering Sciences*, 2008, **366**, 1575–1590.
- 13 J. O. Wolff and S. N. Gorb, *Scientific reports*, 2013, **3**, 1–7.
- 14 K. F. Frost, S. N. Gorb and J. O. Wolff, *Zoologischer Anzeiger*, 2018, **273**, 231–239.
- 15 H. Lee, B. P. Lee and P. B. Messersmith, *Nature*, 2007, **448**, 338–341.
- 16 L. Qu, L. Dai, M. Stone, Z. Xia and Z. L. Wang, *Science*, 2008, **322**, 238–242.
- 17 H. E. Jeong, J.-K. Lee, H. N. Kim, S. H. Moon and K. Y. Suh,

- Proceedings of the National Academy of Sciences*, 2009, **106**, 5639–5644.
- 18 M. Kamperman, E. Kroner, A. del Campo, R. M. McMeeking and E. Arzt, *Advanced Engineering Materials*, 2010, **12**, 335–348.
  - 19 L. O. Prieto-López and J. A. Williams, *Biomimetics*, 2016, **1**, 1–8.
  - 20 B. V., H. R., G. N. K., G. A., M. R. M. and A. E., *Adv. Funct. Mater.*, 2016, **26**, 4687–4694.
  - 21 R. Hensel, K. Moh and E. Arzt, *Adv. Funct. Mater.*, 2018, **28**, 1800865.
  - 22 C. S. Davis, D. Martina, C. Creton, A. Lindner and A. J. Crosby, *Langmuir*, 2012, **28**, 14899–14908.
  - 23 D. Maugis and M. Barquins, *J. Phys. D: Appl. Phys.*, 1978, **11**, 1989 – 2023.
  - 24 K. Shull, E. Kramer, G. Hadziioannou and W. Tang, *Macromolecules*, 1990, **23**, 4780–4787.
  - 25 M. D. Bartlett, A. B. Croll, D. R. King, B. M. Paret, I. D. J. and A. J. Crosby, *Adv. Mater.*, 2012, **24**, 1078–1083.
  - 26 D. L. Blair and A. Kudrolli, *Phys. Rev. Lett.*, 2005, **94**, 166107.
  - 27 E. Sultan and A. Boudaoud, *Phys. Rev. Lett.*, 2006, **96**, 136103.
  - 28 M. Adda-Bedia, A. Boudaoud, L. Boué and S. Deboeuf, *J. Stat. Mech.*, 2010, **2010**, P11027.
  - 29 A. Cambou and N. Menon, *Proc. Nat. Acad. Sci.*, 2011, **108**, 14741–14745.
  - 30 K. Matan, R. B. Williams, T. A. Witten and S. R. Nagel, *Phys. Rev. Lett.*, 2002, **88**, 076101.
  - 31 A. S. Balankin, O. S. Huerta, F. H. Méndez and J. P. Ortiz, *Phys. Rev. E*, 2011, **84**, 021118.
  - 32 G. A. Vliegthart and G. Gompper, *Nat. Mater.*, 2006, **5**, 216–221.
  - 33 T. Tallinen, J. Åström and J. Timonen, *Nat. Mater.*, 2009, **8**, 25–29.
  - 34 S. Deboeuf, E. Katzav, A. Boudaoud, D. Bonn and M. Adda-Bedia, *Phys. Rev. Lett.*, 2013, **110**, 104301.
  - 35 M. Habibi, M. Adda-Bedia and D. Bonn, *Soft Matter*, 2017, **13**, 4029–4034.
  - 36 O. Gottesman, J. Andrejevic, C. H. Rycroft and S. M. Rubinstein, *Comm. Phys.*, 2018, **1**, 70.
  - 37 A. B. Croll, T. Twohig and T. Elder, *Nat. Commun.*, 2019, **10**, 1502.
  - 38 J. Andrejevic, L. M. Lee, S. M. Rubinstein and C. H. Rycroft, *Nat. Commun.*, 2021, **12**, 1470.
  - 39 A. B. Croll, Y. Liao, Z. Li, W. Jayawardana, T. Elder and W. Xia, *Matter*, 2022, **5**, 1792–1805.
  - 40 T. Elder, T. Twohig, H. Singh and A. B. Croll, *Soft Matter*, 2020, **16**, 10611–10619.
  - 41 A. J. Crosby and K. R. Shull, *J. Poly. Sci. B: Poly. Phys.*, 1999, **37**, 3455–3472.
  - 42 H. Lakrout, C. Creton, D. Ahn and K. R. Shull, *Macromolecules*, 2001, **34**, 7448–7458.
  - 43 K. Brown, J. C. Hooker and C. Creton, *Macromol. Mater. Eng.*, 2002, **287**, 163–179.
  - 44 D. R. Darby, Z. Cai, C. R. Mason and J. T. Pham, *Journal of Applied Polymer Science*, 2022, **139**, e52412.
  - 45 B. Persson and E. Tosatti, *J. Chem. Phys.*, 2001, **115**, 5597–5610.
  - 46 B. N. J. Persson, O. Albohr, U. Tartaglino, A. I. Volokitin and E. Tosatti, *Journal of Physics: Condensed Matter*, 2004, **17**, R1–R62.
  - 47 G. A. D. Briggs and B. B. J., *J. Phys. D: Appl. Phys.*, 1977, **10**, 2453–2466.
  - 48 L. Dorogin, A. Tiwari, C. Rotella, P. Mangiagalli and B. N. J. Persson, *Phys. Rev. Lett.*, 2017, **118**, 238001.
  - 49 L. Pastewka and M. O. Robbins, *Proc. Nat. Acad. Sci.*, 2014, **111**, 3298–3303.
  - 50 K. N. G. Fuller and D. Tabor, *Proceedings of the Royal Society of London. A. Mathematical and Physical Sciences*, 1975, **345**, 327–342.
  - 51 G. Palasantzas, *Surface Science*, 2003, **529**, 527–532.
  - 52 B. Persson, *Eur. Phys. J. E*, 2002, **8**, 385–401.
  - 53 A. G. Akulichev, A. Tiwari, L. Dorogin, A. T. Echtermeyer and B. N. J. Persson, *Euro. Phys. Lett.*, 2017, **120**, 36002.